# PERFORMANCE OF POLAR WRF OVER ARCTIC LAND*

Keith M. Hines[1], David H. Bromwich[1,2], Michael Barlage[3], and Andrew G. Slater[4]

[1]Polar Meteorology Group, Byrd Polar Research Center,
The Ohio State University, Columbus, Ohio
[2]Atmospheric Sciences Program, Department of Geography
The Ohio State University, Columbus, Ohio
[3]National Center for Atmospheric Research
[4]Cooperative Institute for Research in Environmental Sciences, University of Colorado

## 1. Introduction

Earlier work with "Polar MM5" a version of the 5th generation Penn State/National Center for Atmospheric Research (NCAR) Mesoscale Model (MM5) demonstrated that regional optimizations specific for the polar regions can yield a much improved performance for both the Arctic and Antarctic applications (e.g., Bromwich et al. 2001, 2003; Cassano et al. 2001; Powers et al. 2003). Consequently, a polar-optimized version of the Weather Research and Forecasting model (WRF) was developed by the Polar Meteorology Group of Ohio State University's Byrd Polar Research Center. Many Arctic and Antarctic applications are relevant for Polar WRF (http://polarmet.mps.ohio-state.edu/PolarMet/pwrf.html). A prime example is daily operational numerical weather prediction to help NSF-supported Antarctic field operations (http://www.mmm.ucar.edu/rt/wrf/amps/, Bromwich et al. 2005; Powers et al. 2003; Powers 2007).

Polar WRF that require regional testing for its boundary layer parameterization, cloud physics, radiation, snow surface physics and sea ice treatment. Developmental simulations consider three types of polar climate regimes: (i) ice sheet areas (Antarctica and Greenland), (ii) polar oceans (especially sea ice surfaces) and (iii) Arctic land. The testing and development work for Polar WRF began with both winter and summer simulations for ice sheet surface conditions using Greenland area domains (Hines and Bromwich 2008). The simulations facilitated improvements to ice sheet surface energy balance and snow firn energy transfer for the Noah land surface model (LSM). Furthermore, work at the NCAR Research Applications Laboratory (RAL) on Noah improvements for the Arctic will result in future improvements to Polar WRF.

*Corresponding Author Address: Keith M. Hines, Byrd Polar Research Center, The Ohio State University, 1090 Carmack Road, Columbus, OH 43210-1002, email: hines.91@osu.edu.

The model is also used for the production of the high-resolution regional reanalysis of known as the Arctic System Reanalysis (Bromwich et al. 2009b). For this application, Polar WRF will have the capability to join the forecast skill of a state-of-the-art mesoscale model with advanced data assimilation techniques under development for WRF-Var (Barker et al. 2004).

## 2. Previous Work

In addition to Greenland-area simulations of Hines and Bromwich (2008), Polar WRF has been tested over the Arctic Ocean in comparison to the highly detailed observations of the Surface Heat Budget of the Arctic Ocean (SHEBA, Persson et al. 2002) during 1997/98. A new addition to Polar WRF was a treatment for grid points containing both open water and sea ice. This was added to the polar-optimized version starting with WRF version 2.2. The fractional sea ice treatment developed by the Polar Meteorology Group is now available to the community as a standard option in the recently released version 3.1 of WRF. The surface layer component of the boundary layer routine is called separately for the ice and liquid portions of a grid box in pack ice. The LSM is then called for the ice portion to obtain the surface fields. In contrast, for the open-water fraction, the surface fluxes are computed by the atmospheric surface boundary layer routine, and the LSM is not invoked there. Net surface fields are obtained by a weighted average of ice and water areas. The new sea ice treatment was tested with the Noah LSM.

The Western Arctic grid for the SHEBA case is shown in Fig. 1. The 141×11 horizontal domain has 25-km resolution, and 28 levels are included in the vertical. Arctic conditions were simulated for the selected months: January 1998, June 1998, and August 1998 representing mid-winter, early summer and late summer conditions, respectively. Very good results were obtained for all three months and the findings are presented in Bromwich et al. (2009a).

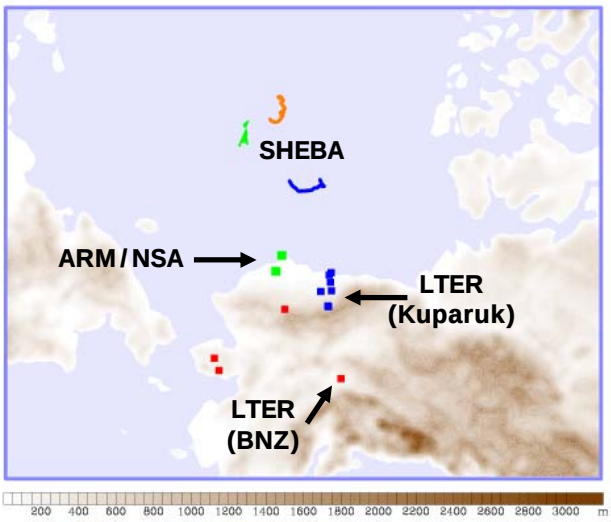


Figure 1. Domain for the Polar WRF simulations of the western Arctic. Squares show selected Arctic land observing stations. Green squares show the locations of Barrow and Atqasuk, Alaska. Marks in the Arctic Ocean show the location of Ice Station SHEBA during January (blue), June (green) and August (red) 1998.

## 3. Arctic Land Simulations

The current study, representing the third of the three stages of evaluation of Polar WRF for Arctic surface types, prioritizes results over land for Arctic simulations. For this study, the polar optimizations are added to WRF version 3.0.1.1. Simulations are run with a similar procedure as in Bromwich et al. (2009a) with a series of 48-hr integrations starting each day at 0000 UTC for the study period from 15 November 2006 until 30 July 2007, including part of the International Polar Year (IPY). Atmospheric initial and boundary conditions every 6 hours are adapted from the Global Forecasting System (GFS, Global Climate and Weather Modeling Branch, 2003) model of the National Centers for Environmental Prediction. Sea ice fraction is obtained from AMSR-E retrievals available from the National Snow and Ice Data Center (NSIDC).

Due to the slow spin-up of soil variables in the LSM, a continuous simulation of soil temperature and moisture within the unified Noah LSM is performed through cycling the 48-hr soil output into the WRF initial conditions at the appropriate valid times. Initial soil conditions for 15 November 2006 are taken from a 10-yr High-Resolution Land Data Assimilation (HRLDAS, Chen et al. 2007) run performed by the third author at NCAR. The deep soil temperature is taken from a database of the mean annual temperature at the bottom of the phase change boundary compiled by the fourth author at the Cooperative Institute for Research in Environmental Sciences (CIRES) and NSIDC.

The same western Arctic grid as in Bromwich et al. (2009a) is used for these simulations (Fig. 1). In the vertical, 28 sigma levels extend from the surface to 10 hPa, with the lowest 10 layers centered approximately at 14, 42, 75, 118, 171, 238, 325, 433, 561, and 748 m, respectively above ground level. The initial spin-up time for the atmospheric simulation set at 24 hours, and the model output from hours 24-45 is combined into multi-month fields.

Over the Arctic pack ice, the ice surface conditions show significant season changes. Therefore, following Bromwich et al. (2009a), sea ice albedo is specified at 0.82 until the onset of spring/summer melt. Sea ice albedo then decreases linearly in time over 35 days until reaching a value of 0.5. During July, the sea ice albedo changes linearly in time from 0.5 (representing a mix of bare ice and developing melt ponds) to 0.65 at the end of the month (when the melt ponds are deeper and taken to be represented as part of the open-water fraction). The onset of snow melt over sea ice is taken as a function of latitude and julian day for 2007 from a dataset provided by Mark Anderson of the University of Nebraska-Lincoln.

The albedo of snow over land is taken as 0.8 until the onset of the snowmelt transition. The onset is estimated as a function of latitude varying from 21 April in the southern part of the domain until early June for the northernmost land grid points within the domain. The snow albedo is taken to rapidly change from 0.8 to 0.65 during the transition specified to be 5 days long.

Simulation results are compared to climatological observing sites of the Atmospheric Research Measurement North Slope of Alaska (NSA) sites at Barrow, AK (71.3233°N, 156.6158°W, 7.6 m ASL) and Atqasuk, AK (70.4720°N, 157.4081°W, 20 m ASL), and the Long Term Ecological Research (LTER) sites including the forested region in central Alaska at Bonanza Creek, AK and northern tundra sites near the Kuparuk River Basin.

## 4. Results

Figure 2 shows time series of 2-m temperature. The observations are from the Atmospheric Research Measurement North Slope of Alaska (NSA) site Barrow, AK. The nearest Polar WRF grid point over land to Barrow has a land use type of mixed tundra. The first panel covers the time period from 26 December 2006 to 25 April 2007. The second panel is for 5 April to 3 August. Good agreement is shown between the

simulated and observed temperature for synoptic variability and seasonal change until the snow melts at the end of May 2007. The biases from January to May are less than 2°C in magnitude for each month at Barrow (Fig. 3a). Larger positive biases are seen inland at Atqasuk. After the snow cover melts maximum daytime temperature frequently exceed observed values by about 10°C during June and July. The bias for June is 5.0°C and that for July is 3.1°C. The influence of the adjacent Arctic Ocean at Barrow, however, probably has a strong impact on the positive bias for Polar WRF. At the NSA site Atqasuk, located several grid points south of the coastline, the bias is smaller, 2.8°C for June and only 0.1°C for July. Results in northeastern Alaska in the Kuparuk River basin (not shown) suggest a positive bias there. In contrast, comparison of simulated temperature for forested regions in central Alaska to the LTER observations at Bonanza Creek (not shown) suggest that the summer diurnal cycle of temperature is very well captured there.

Figure 4 shows time series of 10-m wind speed for observations at Barrow and model results. During winter and spring, the model qualitatively captures the variability of wind speed at Barrow, with a few exceptions. Barrow tends to have higher maximum speeds than are found for the model as seen in Fig. 4. Similar results are seen at Atqasuk. Thus, the biases vary from -0.3 to -1.2 m $s^{-1}$ during the winter and spring months (Fig. 3b). The wind speed biases are reversed in sign during the summer months, indicative of highly different regimes between snow-covered and snow-free months. The tendency to simulate smaller than observed wind speed is also seen at Atqasuk (not shown).

## 5. Summary and Comments

The development of Polar WRF provides an improved model for Arctic and Antarctic climate and synoptic applications. Following the path used to develop Polar MM5, testing began with simulations of the Greenland Ice Sheet region (Hines and Bromwich 2008). The second phase of testing was a comparison of Polar WRF simulations to observations over the Arctic pack ice at SHEBA. The current study shows the test results for the third phase. Polar WRF simulations based upon WRF version 3.0.1.1 are compared to land observations from the western Arctic. Work continues on enhancement of Polar WRF for the Arctic System Reanalysis. Planned future enhancements to Polar WRF include adding variable sea ice thickness, and improving the thermodynamic treatment of snow over sea ice.

*ACKNOWLEDGMENTS.* This research is supported by NSF IPY Grant 0733023, NASA Award NNG04GM26G, and DOE Award GRT00008066.

## 6. REFERENCES

Barker, D., W. Huang, Y. Guo, and Q. Xiao, 2004: A Three-dimensional (3DVAR) data assimilation system for use with MM5. Implementation and initial results. *Mon. Wea. Rev.*, **132,** 897-914.

Bromwich, D.H., J.J. Cassano, T. Klein, G. Heinemann, K.M. Hines, K. Steffen, and J.E. Box, 2001: Mesoscale modeling of katabatic winds over Greenland with the Polar MM5. *Mon. Wea. Rev.*, **129,** 2290-2309.

Bromwich, D.H., A.J. Monaghan, J.G. Powers, J.J. Cassano, H. Wei, Y. Kuo, and A. Pellegrini, 2003: Antarctic Mesoscale Prediction System (AMPS): A case study from the 2000/2001 field season. *Mon. Wea. Rev.*, **131,** 412-434.

Bromwich, D.H., A.J. Monaghan, K.W. Manning, and J.G. Powers 2005: Real-time forecasting for the Antarctic Mesoscale Prediction System (AMPS). *Mon. Wea. Rev.*, **133,** 579-603.

Bromwich, D.H., K.M. Hines, and. L.-S. Bai, 2009a: Developments and Testing of Polar Weather Research and Forecasting model: 2. Arctic Ocean. *J. Geophys. Res*., **114,** D08122, doi:10:1029/2008JD010300.

Bromwich, D.H. and Co-authors, 2009b: A multi-year Arctic System Reanalysis. Preprints, *10th Conf. Polar Meteorology and Oceanography*, 17-21 May 2009, Madison, WI.

Cassano, J.J., J.E. Box, D.H. Bromwich, L. Li, and K. Steffen, 2001: Evaluation of Polar MM5 simulations of Greenland's atmospheric circulation. *J. Geophys. Res.*, **106,** 33,867-33,889.

Chen, F., and Co-authors, 2007: Description and evaluation of the characteristics of the NCAR High-Resolution Land Data Assimilation system. *J. Appl. Meteor. Clim.,* **46,** 694-713.

Global Climate and Weather Modeling Branch, 2003: The GFS Atmospheric Model. *NCEP Office Note 442,* 14 pp. [Available from http://www.emc.noaa.gov/officenotes/newernotes/on442.pdf]

Hines, K.M., and D.H. Bromwich, 2008: Development and testing of Polar WRF. Part I. Greenland ice sheet meteorology. *Mon.Wea.Rev.,* **136,** 1971-1989.

Persson, P.O.G., C.W. Fairall, E.L. Andreas, P.S. Guest and D.K. Perovich, 2002: Measurements near the Atmospheric Surface Flux Group Tower at SHEBA: Near-surface conditions and surface energy budget. *J. Geophys. Res.*, **107,** 8045, doi:10.1029/2000JC000705.

Powers, J.G., A.J. Monaghan, A.M. Cayette, D.H. Bromwich, Y-H. Kuo, and K.W. Manning, 2003: Real-time mesoscale modeling over Antarctica: The Antarctic Mesoscale Prediction System (AMPS). *Bull. Amer. Meteor. Soc*., **84,** 1533-1545.

Powers, J.G., 2007: Numerical prediction of an Antarctic severe wind even with the weather research and forecasting (WRF) model. *Mon. Wea. Rev*., **135,** doi:10:1175/MWR3459.1, 3134-3157.

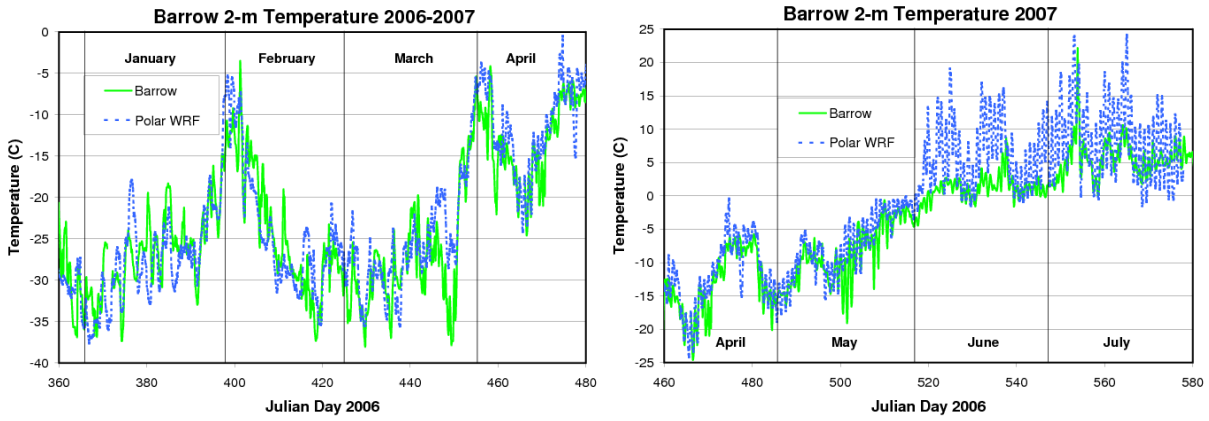


Figure 2. Time series 2-m temperature (°C) from observations at Barrow, AK and the nearest Polar WRF land grid point. The horizontal axis shows the julian day starting from 1 January 2006.

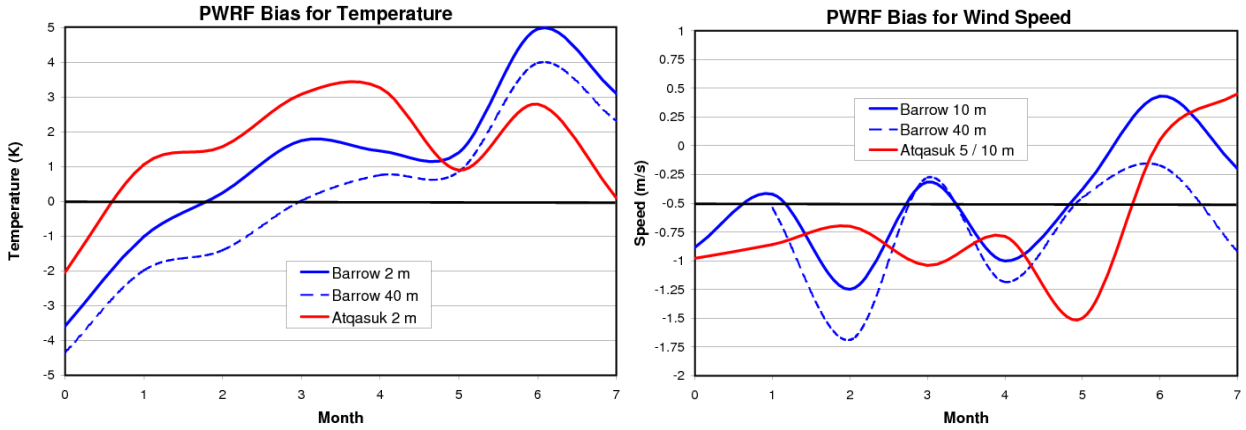


Figure 3. Monthly bias or 2-m temperature (K) and 10-m wind speed (m $s^{-1}$) at Barrow, AK (blue lines) and Atqasuk, AK (red lines). The bias at 40-m for Barrow is shown by the dashed blue lines. The horizontal axis shows the month for 2007, with the zero value for December 2006.

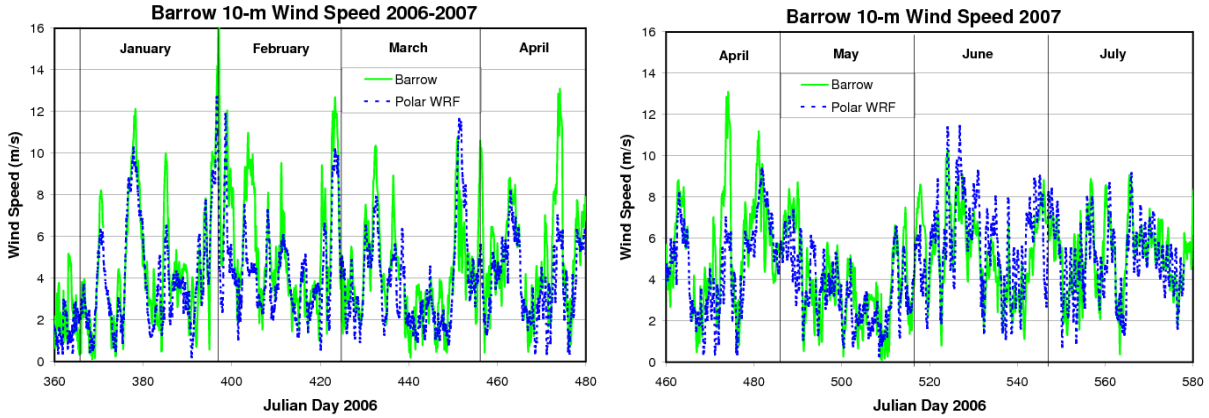


Figure 4. Time series 10-m wind speed (m $s^{-1}$) from observations at Barrow, AK and the nearest Polar WRF land grid point. Horizontal axis as in Fig. 2.